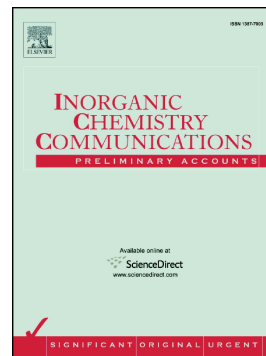


Accepted Manuscript

A bi-functional 3D PbII–organic framework for Knoevenagel condensation reaction and highly selective luminescent sensing of Cr2O7²⁻

Miaochao Lin



PII: S1387-7003(19)30352-1
DOI: <https://doi.org/10.1016/j.inoche.2019.04.042>
Reference: INOCHE 7386
To appear in: *Inorganic Chemistry Communications*
Received date: 8 April 2019
Revised date: 27 April 2019
Accepted date: 27 April 2019

Please cite this article as: M. Lin, A bi-functional 3D PbII–organic framework for Knoevenagel condensation reaction and highly selective luminescent sensing of Cr2O7²⁻, *Inorganic Chemistry Communications*, <https://doi.org/10.1016/j.inoche.2019.04.042>

This is a PDF file of an unedited manuscript that has been accepted for publication. As a service to our customers we are providing this early version of the manuscript. The manuscript will undergo copyediting, typesetting, and review of the resulting proof before it is published in its final form. Please note that during the production process errors may be discovered which could affect the content, and all legal disclaimers that apply to the journal pertain.

A bi-functional 3D Pb^{II}-organic framework for Knoevenagel condensation reaction and highly selective luminescent sensing of Cr₂O₇²⁻

Miaochao Lin,^{a*}

^a *Department of Chemistry Chemical Engineering, Xinxiang University, Xinxiang 453003, China.*

Corresponding Authors: Miaochao Lin

E-mail address: linmcxxu@sina.com

Abstract

A novel 3D Pb^{II}-organic framework {Pb(AIA)₂}_n (denoted as **1**) can be successfully constructed by the assembly of 5-aminonicotinic acid (HAIA) and Pb^{II} cation under hydrothermal condition. The prepared **1** can be investigated and characterized by many technologies, including single-crystal X-ray diffraction, powder X-ray diffraction, luminescent spectrum, elemental analysis (C, H, and N), UV-Vis spectrum, as well as thermogravimetric analysis, respectively. The resultant **1** has lots of uncoordinated pyridine nitrogen atoms and -NH₂ in the structure, which can be commonly considered as Lewis basic sites to catalysis Knoevenagel condensation reaction. Meanwhile, the as-synthesized **1** with the luminescent property can be considered as a luminescent sensor for selective sensing of Cr₂O₇²⁻ with excellent recyclability at least reusing four runs.

Keywords: Pb^{II}-organic framework; catalysis; luminescent sensor; recyclability; Cr₂O₇²⁻.

Materials are the most important and hot topic in our world, because they always directly affect and change many research fields. Recently, metal-organic frameworks (namely MOFs)^[1-4] have been developed and explored rapidly as a novel class of inorganic-organic hybrid material by lots of material scientists and chemists, not only because of their interesting and various constructions,^[5-7] but also thanks to their extensive applications, including gas sorption/separation,^[8-10] luminescent sensor,^[11-13] heterogeneous catalysis,^[14-16] biological enzyme or drug loading,^[17-19] and optical material.^[20,21] Meanwhile, designability and controllability of MOFs directly promote the booming development in all materials. Design and synthesis of novel MOFs with targeted functional properties is still very important and interesting in this field, attracting huge number of interests from many scientists. Actually, MOFs are crystal materials and constructed by the coordination between metal cations and organic linkers.^[22-24] Hence, MOFs can be fabricated by using different linkers, metal cations, and assemble conditions.^[25-27] Among all application areas, heterogeneous catalysis

and luminescent sensor both have been widely investigated for MOF materials due to their important practical meanings and potential applications. Luminescent MOFs with various luminescent sources have lots of superior properties for naked-eye visibility, fast response, high selectivity, and excellent recyclability.^[28-30] As we know, $\text{Cr}_2\text{O}_7^{2-}$ is a widely used and strong oxidant with high toxic and corrosive in the laboratory and industry. The excess of $\text{Cr}_2\text{O}_7^{2-}$ will significantly endanger human being's health and ecological environment, for example gastrointestinal problem, ecological risk, cardiovascular failure, skin irritation, as well as respiratory infection.^[31,32] Hence, it is important to design and prepare useful sensor materials to detect $\text{Cr}_2\text{O}_7^{2-}$ precisely for environmental conservation and health of human beings. Furthermore, Knoevenagel condensation reaction is a classical organic synthesis reaction, which is widely used in many industry fields and always applied to estimate the catalytic performance of catalysis.^[33,34]

In this work, we selected a rigid linker 5-aminonicotinic acid (denoted as HAIA), which can be successfully assembled with Pb^{II} cation to construct a novel three-dimensional (3D) framework $\{\text{Pb}(\text{AIA})_2\}_n$ (namely **1**). The resultant crystals were generated finally by heating HAIA, $\text{Pb}(\text{OAc})_2$, and NaOH in MeCN at 120 °C for three days under hydrothermal synthesis.^[35] The achieved sample was studied by single-crystal X-ray diffraction, powder X-ray diffraction (PXRD), elemental analysis of C, H, and N, thermogravimetric analysis (TGA), UV-Vis spectrum, and luminescent property. Due to the luminescent property and various Lewis basic sites (uncoordinated pyridine nitrogen atoms and $-\text{NH}_2$) in the structure, the resultant MOF **1** not only can be considered as Lewis basic catalyst for Knoevenagel condensation reaction with good catalytic effect and recyclability, but also as a luminescent sensor toward $\text{Cr}_2\text{O}_7^{2-}$ with excellent selectivity and reusability.

Single-crystal X-ray diffraction result obviously shows that MOF **1** crystallizes in the triclinic crystal system and $P\bar{1}$ space group.^[36] As depicted in Fig. 1a, the asymmetric unit of as-synthesized **1** contains one independent Pb^{II} cation and two

completely deprotonated AIA⁻ linkers. As shown in Figs. 1b and 1c, there are two different coordination modes of AIA⁻ linker in MOF **1**. The linker in mode I is coordinated with three different Pb^{II} cations by $\mu_3-\eta^1: \eta^2: \eta^1$; meanwhile the linker in mode II can be linked with three Pb^{II} cations as $\mu_3-\eta^1: \eta^1: \eta^1$. The ration of mode I and mode II is 1 : 1 in the whole structure. More interestingly, the free pyridine ring exists in mode I, and uncoordinated -NH₂ group retains in mode II, which both can be considered as functional sites for the potential applications. As seen in Fig. 1d, the coordination environment of Pb^{II} cation is seven-coordinated with five O-donors from one bidentate and three monodentate carboxylic groups from four different AIA⁻ bridging linkers, one -NH₂ group and one pyridine ring from two AIA⁻ linkers (Pb-O = 2.4452 – 2.7737 Å and Pb-N = 2.6407 – 2.7135 Å). In addition, two neighboring Pb^{II} cations can be connected by each other through the carboxylic groups to construct a bi-nuclear Pb cluster in Fig. 1d. The Pb···Pb distance in this cluster is about 3.1735 Å. Terminally, a novel 3D coordinated construction was successfully fabricated by the coordinated force between these organic linkers and Pb^{II} centers (Figs. 1e-1g).

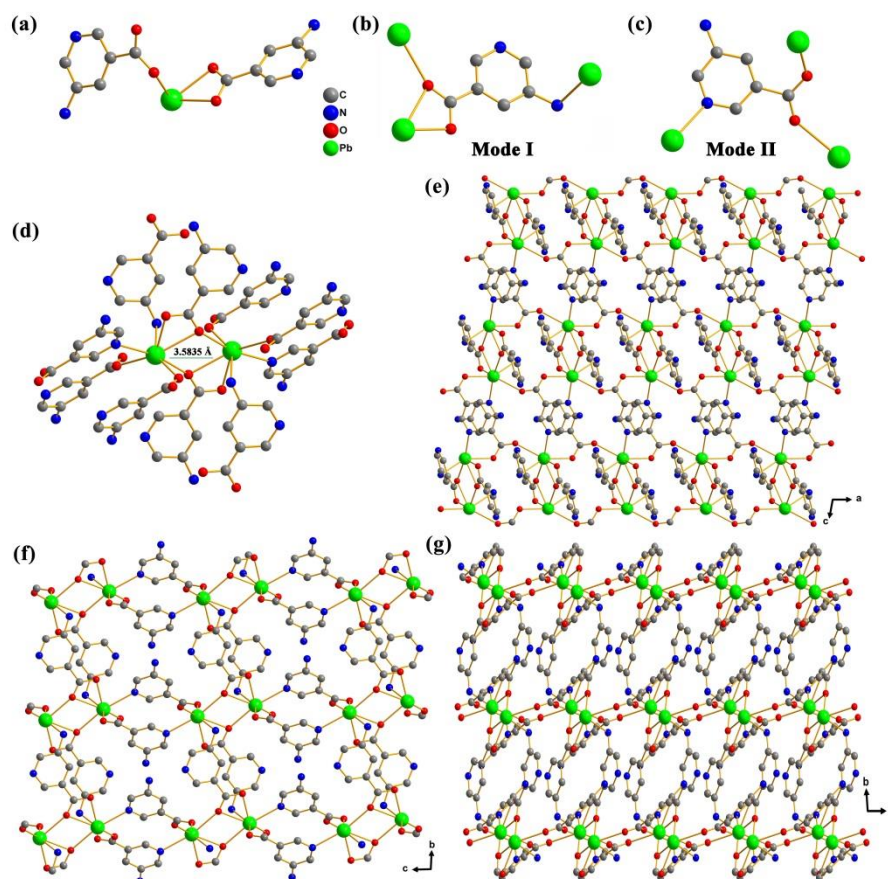


Fig. 1. (a) The asymmetric unit of as-synthesized **1**; (b and c) the coordination modes of bridging organic linkers; (d) the coordination environment of Pb^{II} ; and (e-g) viewing of the 3D construction of **1** (all hydrogen atoms are removed for clarity, and C, gray; N, blue; O, red; and Pb, green).

As shown in Fig. 2a, PXRD profile of as-synthesized MOF **1** was carefully measured in air at room temperature. The data of experimental sample was consistent with those of the simulated pattern from its single-crystal data, which clearly illustrated that the prepared block samples are the same with the single-crystal structure and pure phase. On the other hand, TGA data of the as-synthesized **1** was measured in air from indoor temperature to 800 °C carefully. The results exhibited that the framework can keep well to 300 °C, and a significant weight loss from 350°C because of the organic linker decomposition (Fig. 2b).

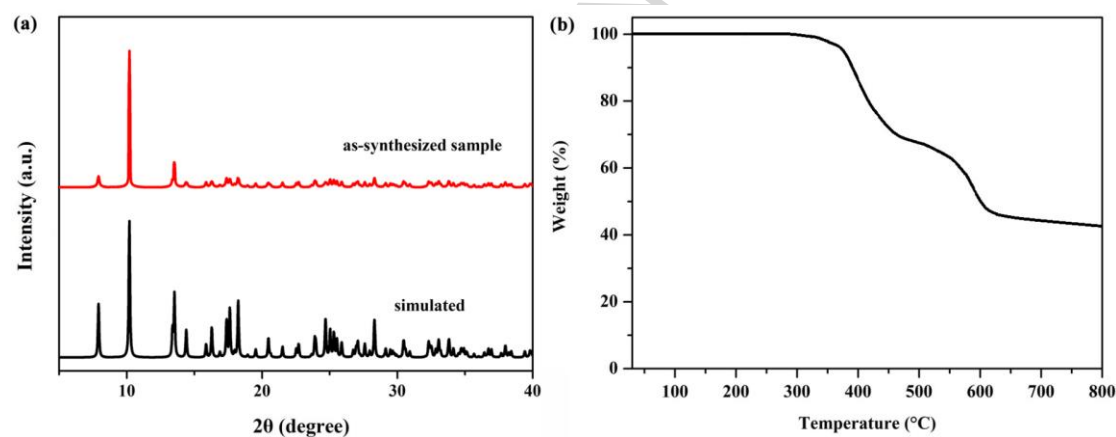


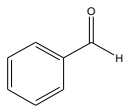
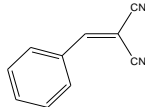
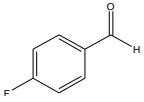
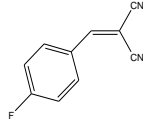
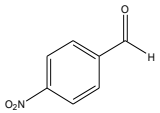
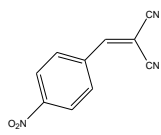
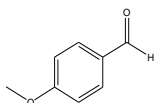
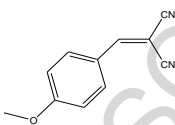
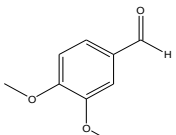
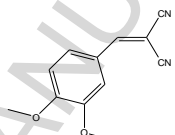
Fig. 2. (a) PXRD data of simulated (black) and as-synthesized **1** (red); and (b) the corresponding TGA data of fresh sample in air.

Due to various Lewis basic sites (uncoordinated pyridine nitrogen atoms and $-\text{NH}_2$) in MOF **1**, the resultant sample can be investigated as an efficient basic catalyst. Knoevenagel condensation reaction was studied in detail as a research model (Table 1).^[37-39] Prior this reaction, experimental MOF **1** was immersed into fresh toluene for 12 hours and further dried in air. In this typical trial, substrate with different functional groups (1 mmol), malononitrile (1.1 mmol), and catalyst (MOF **1**, 100 mg) with toluene (6 mL) were mixed together in a glass reactor. This mixture was directly heated at a constant temperature at 85 °C for 4 hours in an oil bath. The finally yields

can be easily made sure and calculated by the gas chromatography. All catalytic data of these Knoevenagel condensation reactions with different aldehyde substrates were summarized in Table 1. As seen in entry 1, the yield of the targeted product 2-benzylidenemalononitrile product can reach up about 100%, which was further selected as a reaction model to study the corresponding kinetic catalytic effect at different reaction times (Fig. 3a). The obtained kinetic catalytic result obviously displayed that the organic reaction almost reacted completely within 4 hours. To investigate the necessary of catalyst **1**, the reaction was stopped quickly after removing **1**. In addition, it is found that the catalytic yield was only about 6% without catalyst **1** (entry 2). The above result evidently demonstrated that catalytic **1** plays a significantly important role for this reaction. Furthermore, several substituted aldehyde reactants were used to discuss and investigate the different performances in the presence of MOF **1**. As illustrated in entries 3 and 4, these corresponding catalytic results shown that the excellent yields (>99%) were both founded for withdrawing groups (-F and -NO₂). However, the yields of aldehyde with electron-donor groups decreased significantly. One -OMe group in entry 5 and two -OMe groups in entry 6 both decreased to 87 and 74, respectively. Due to the no-porous structure, the low catalytic is not caused by the size diffusion or selectivity.

Table 1. All results of Knoevenagel condensation reactions based on different aldehyde substrates.

Entry	Substrate	Product	Yield (%)
1			>99

2			6
3			>99
4			>99
5			87
6			74

Notably, it is very important to easily recollect and regenerate for the heterogeneous catalysis. For these reactions, MOF **1** can be feasibly separated and collected by simply centrifuging at 8500 r·min⁻¹ about 3 minutes, which can be further regenerated after washing with fresh toluene. As founded in Fig. 3b, catalytic yields of regenerated **1** after different runs were almost no any change in virtue of the stability of MOF **1**. The PXRD profile of MOF **1** after recycling four times clearly illustrated that the whole network of MOF **1** can keep very well during the catalytic reaction in Fig. S1.

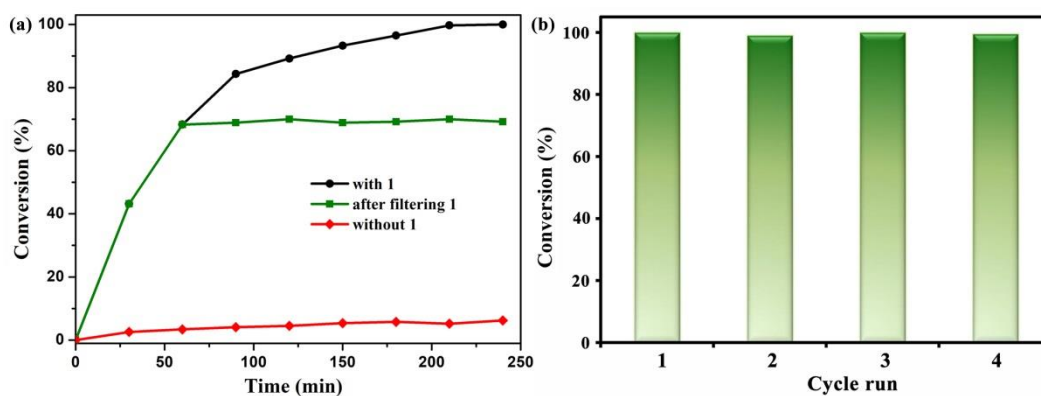


Fig. 3. (a) The kinetics analysis of Knoevenagel condensation reaction; and (b) the reusability of **1**.

As depicted in Fig. 4a, luminescent spectra of free HAIA linker and fresh sample **1** in solid state were both measured and collected at room temperature due to their sensor applications of Pb^{II} -organic frameworks.^[40] The as-synthesized **1** has a broad emission band at 395 nm under excitation 332 nm, which is very similar with that of free linker (406 nm). It is obviously found that the maximum emission band of as-synthesized **1** exhibits slight blue-shift performance compared with that of free HAIA linker. According to the reported literatures, it may be mainly attributed to enhancing the rigidity of bridging linker after coordinating to Pb^{II} cation to decrease the energy loss.^[41] In virtue of MOF **1**'s luminescence, we tried to investigate the luminescent detection capability of **1**. As seen in Fig. 4b, the luminescent intensities of ground MOF **1** are significantly dependent on various solvent molecules. MOF **1** exhibits good luminescent property and insolubility in DMF; meanwhile, the luminescent intensity can retain well even soaking in DMF for one day (Fig. 4c). Hence, all luminescent sensing trials were measured and collected in DMF at room temperature. More importantly, the recycled PXRD pattern of regenerated MOF **1** can preserve its whole structure in DMF for one day (Fig. 4d).

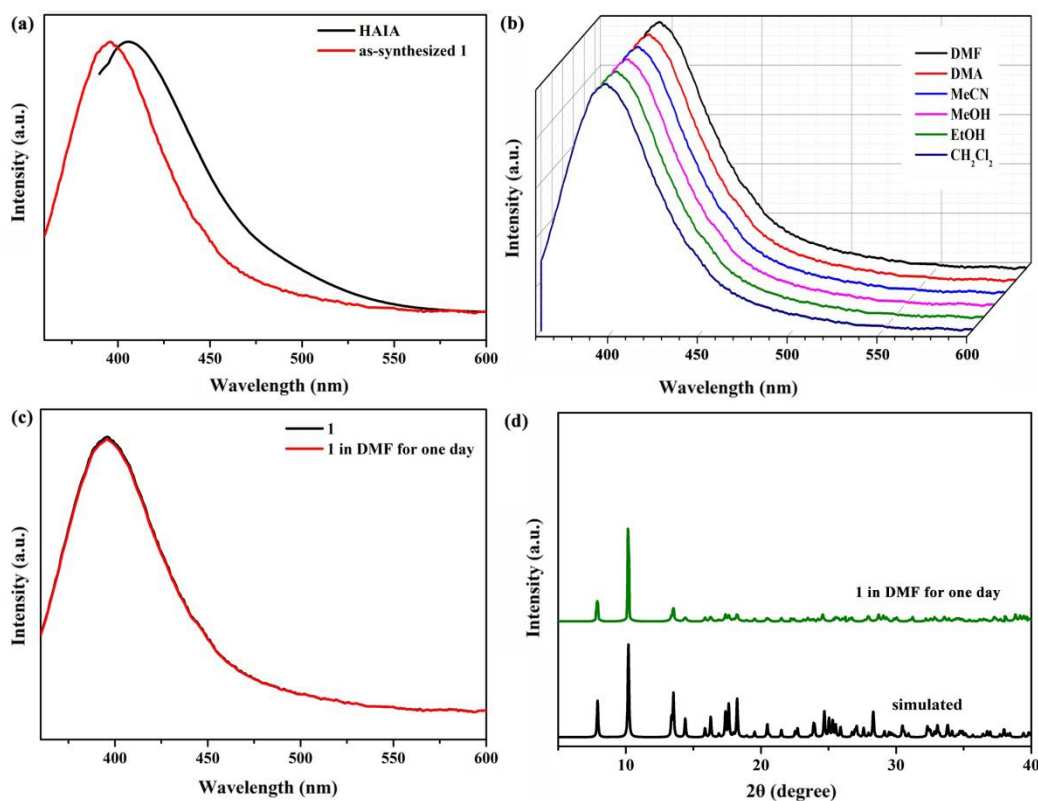


Fig. 4. (a) Solid-state luminescent spectra of free linker and as-synthesized **1**; (b) luminescent spectra of **1** in different solvents; (c) the emission intensity and (d) PXRD pattern of MOF **1** after soaking in DMF for one day.

The ground crystals (1.0 mg L^{-1}) were ultrasonically dispersed in fresh DMF with KX ($X = \text{F}^{-}, \text{Cl}^{-}, \text{Br}^{-}, \text{ClO}_3^{-}, \text{BrO}_3^{-}, \text{IO}_3^{-}, \text{CrO}_4^{2-}$ and $\text{Cr}_2\text{O}_7^{2-}$, $5.0 \times 10^{-4} \text{ mol L}^{-1}$), which were collected their corresponding luminescent spectra after two minutes. The results evidently exhibited that the luminescent intensities of ground MOF **1** were almost no changes in $\text{F}^{-}, \text{Cl}^{-}, \text{Br}^{-}, \text{ClO}_3^{-}, \text{BrO}_3^{-}, \text{IO}_3^{-}$, and CrO_4^{2-} , while **1** happened obvious luminescent quenching performance in $\text{Cr}_2\text{O}_7^{2-}$ solution (Fig. 5a). It obviously stated that MOF **1** is a greatly potential luminescence sensor to $\text{Cr}_2\text{O}_7^{2-}$. The titration experiments were implemented to quantitatively appraise the detection capability of MOF **1** toward $\text{Cr}_2\text{O}_7^{2-}$ in detail. As illustrated in Fig. 5b, the intensity of MOF **1** obviously reduced with the increasing $\text{Cr}_2\text{O}_7^{2-}$ concentration. As we know, the detectability of sensors can be quantitatively calculated by the quenching constant (namely K_{sv}) from Stern-Volmer equation: $(I_0/I) = K_{\text{sv}}[M] + 1$. $[M]$ is the molar

concentration of targeted analyte; meanwhile I_0 and I are on behalf of luminescent intensities of MOF **1** without and with analytes, respectively. As displayed in Fig. 5c, the calculated K_{sv} value is about $1.14 \times 10^4 \text{ M}^{-1}$, which can be calculated by the value of $I_0/I - 1$ and the concentration of $\text{Cr}_2\text{O}_7^{2-}$ in the low concentration range below $3.7 \times 10^{-5} \text{ mol L}^{-1}$ with a good linear relationship $R^2 = 0.9945$. Meanwhile, the calculated detection limit can be calculated from $3\delta/\text{Slope}$ (δ : standard error) and the detection limit of $\text{Cr}_2\text{O}_7^{2-}$ is $1.03 \times 10^{-5} \text{ mol L}^{-1}$. Fig. 5d obviously shown that the luminescent spectra of ground **1** can keep the original intensity in most of anions (F^- , Cl^- , Br^- , ClO_3^- , BrO_3^- , IO_3^- , and CrO_4^{2-}), while the emission intensity could quench quickly once adding $\text{Cr}_2\text{O}_7^{2-}$ in the above mixed solution. The experiments directly illustrated that as-synthesized MOF **1** has the excellent selectivity for $\text{Cr}_2\text{O}_7^{2-}$.

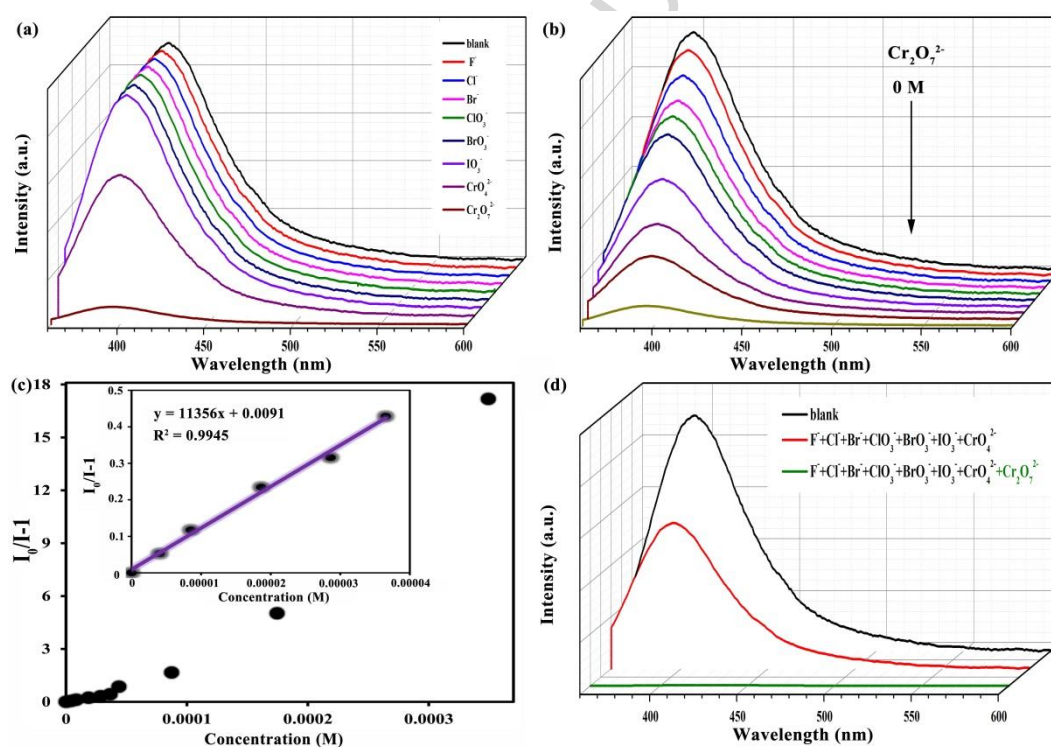


Fig. 5. (a) Luminescent spectra of **1** in different negative anions; (b) luminescent intensities of MOF **1** at different concentrations of $\text{Cr}_2\text{O}_7^{2-}$; (c) Stern-Volmer plots and (d) selective experiments of **1** for $\text{Cr}_2\text{O}_7^{2-}$ in mixed negative anions.

Furthermore, the reusability of MOF **1** can be estimated by using recycle experiments. Reused sample can be directly regenerated and recollected by

centrifugation and washing with DMF several times. As illustrated in Fig. 6a, the regenerated crystals keep their luminescent detection capability even reusing four runs. The response rates of MOF **1** to $\text{Cr}_2\text{O}_7^{2-}$ can be monitored at different time intervals. It is easily founded that ground **1** can fastly achieve the minimum intensity and preserve for a long time, illustrating that the quenching performance is not caused by guest capture (Fig. 6b). From UV-Vis absorption spectra of these chosen negative anions, it shown that only $\text{Cr}_2\text{O}_7^{2-}$ anion has an obviously overlap with the excitation spectrum of MOF **1** (Fig. 6c). Hence, the quenching mechanism may be possibly ascribed to the excitation energy competitive between MOF **1** and $\text{Cr}_2\text{O}_7^{2-}$.^[42,43] In addition, the PXRD result of sample **1** after continuously using four runs proved that the entire network can be kept well for the sensor process (Fig. 6d). Furthermore, the FT-IR spectra of reused samples after four times are consisting with the fresh sample to prove the structural stability (Fig. S2).

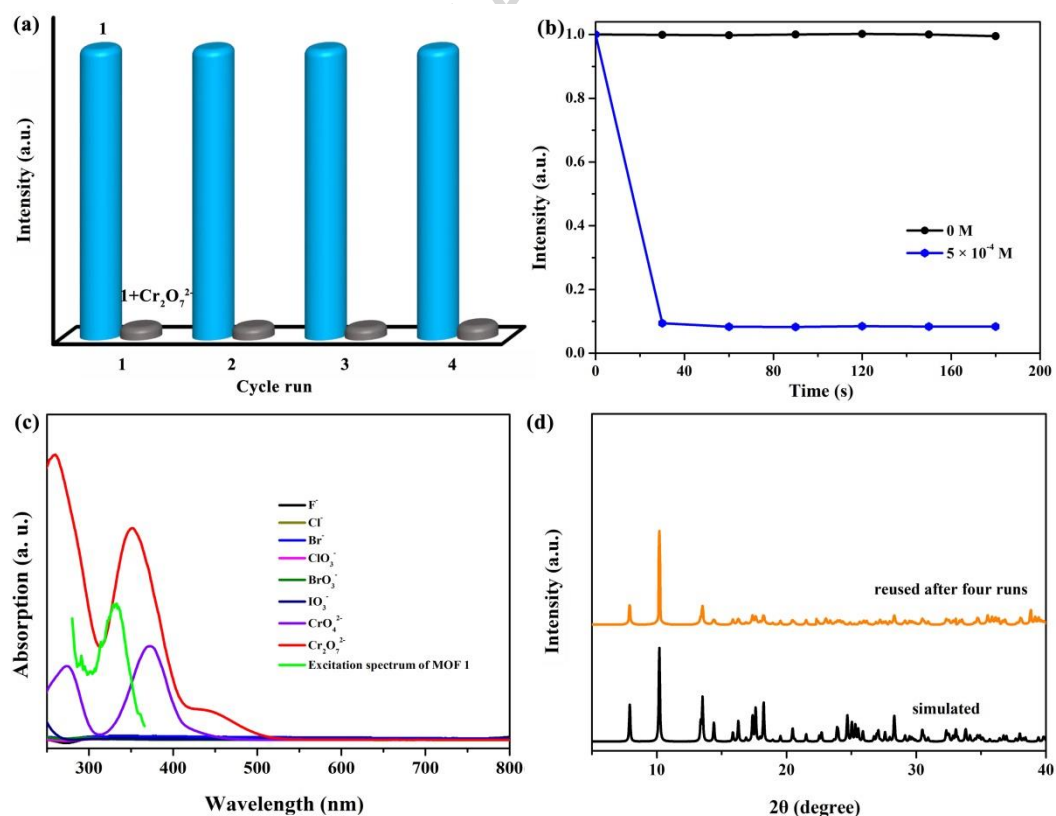


Fig. 6. (a) Reusability of **1** for $\text{Cr}_2\text{O}_7^{2-}$ (5.0×10^{-4} mol L^{-1}); (b) luminescent response rates of **1** toward $\text{Cr}_2\text{O}_7^{2-}$ at different time intervals; (c) UV-Vis spectra for the selected anions; and (d) the

PXRD profile of **1** after reusing four runs.

In conclusion, a 3D Pb^{II}-organic framework can be successfully constructed based on HAIA linker under hydrothermal condition, which has lots of uncoordinated pyridine nitrogen atoms and -NH₂ in the structure to use as a Lewis basic catalyst to catalysis Knoevenagel condensation reaction. Meanwhile, as-synthesized **1** can be considered as a luminescent sensor for Cr₂O₇²⁻ with excellent selectivity. In addition, as-synthesized **1** has outstanding reusability at least four runs.

References

- [1] W.-M. Liao, J.-H. Zhang, Z. Wang, Y.-L. Lu, S.-Y. Yin, H.-P. Wang, Y.-N. Fan, M. Pan, C.-Y. Su, Semiconductive amine-functionalized Co(II)-MOF for visible-light-driven hydrogen evolution and CO₂ reduction, *Inorg. Chem.* 57 (2018) 11436–11442.
- [2] A. Kirchon, L. Feng, H. F. Drake, E. A. Joseph, H.-C. Zhou, From fundamentals to applications: a toolbox for robust and multifunctional MOF materials. *Chem. Soc. Rev.* 47 (2018) 8611–8638.
- [3] H. He, J. A. Perman, G. Zhu, S. Ma, Metal-organic frameworks for CO₂ chemical transformations, *Small* 12 (2016) 6309–6324.
- [4] L. Zhu, X.-Q. Liu, H.-L. Jiang, L.-B. Sun, Metal-organic frameworks for heterogeneous basic catalysis, *Chem. Rev.* 117 (2017) 8129–8176.
- [5] H.-B. Yuan, L. Fu, L.-J. Chen, B. Li, The effect of coordination habits of metal ions on fabricating metal-organic frameworks with thiophenedicarboxylate, *Inorg. Chem. Commun.* 101 (2019) 81–86.
- [6] C. Chen, M. Zhang, W. Zhang, J. Bai, Stable amide-functionalized metal-organic framework with highly selective CO₂ adsorption, *Inorg. Chem.* 58 (2019) 2729–2735.
- [7] Y. Wang, H. Cao, B. Zheng, R. Zhou, J. Duan, Solvent- and pH-dependent

- formation of four zinc porous coordination polymers: framework isomerism and gas separation, *Cryst. Growth Des.* 18 (2018) 7674–7682.
- [8] Y. Wang, X. Wang, X. Wang, X. Zhang, W. Fan, D. Liu, L. Zhang, F. Dai, D. Sun, Effect of functional groups on the adsorption of light hydrocarbons in fmj-type metal–organic frameworks, *Cryst. Growth Des.* 19 (2019) 832–838.
- [9] B. Ugale, S. S. Dhankhar, C. M. Nagaraja, Exceptionally stable and 20-connected Lanthanide metal-organic frameworks for selective CO₂ capture and conversion at atmospheric pressure, *Cryst. Growth Des.* 18 (2018) 2432–2440.
- [10] Y. Zhang, L. Wang, M. Zeng, M. Kurmoo, Fabrication of a capillary column coated with the four-fold-interpenetrated MOF Cd(D-Cam)(tmdpy) for gas chromatographic separation, *Inorg. Chem. Commun.* 83 (2017) 123–126.
- [11] X. Zhao, S. Wang, L. Zhang, S. Liu, G. Yuan, 8-hydroxyquinolate-based metal–organic frameworks: synthesis, tunable luminescent properties, and highly sensitive detection of small molecules and metal ions, *Inorg. Chem.* 58 (2019) 2444–2453.
- [12] Z.-W. Zhai, S.-H. Yang, M. Cao, L.-K. Li, C.-X. Du, S.-Q. Zang, Rational design of three two-fold interpenetrated metal–organic frameworks: luminescent Zn/Cd-metal–organic frameworks for detection of 2,4,6-trinitrophenol and nitrofurazone in the aqueous phase, *Cryst. Growth Des.* 18 (2018) 7173–7182.
- [13] P. C. Rao, S. Mandal, Europium-based metal–organic framework as a dual luminescence sensor for the selective detection of the phosphate anion and Fe³⁺ ion in aqueous media, *Inorg. Chem.* 57 (2018) 11855–11858.
- [14] H. He, Q. Sun, W. Gao, J. A. Perman, F. Sun, G. Zhu, B. Aguila, K. Forrest, B. Space, S. Ma, A stable metal–organic framework featuring a local buffer environment for carbon dioxide fixation, *Angew. Chem., Int. Ed.* 57 (2018) 4657–4662.
- [15] L. Zhu, X.-Q. Liu, H.-L. Jiang, L.-B. Sun, Metal–organic frameworks for heterogeneous basic catalysis, *Chem. Rev.* 117 (2017) 8129–8176.
- [16] Y. Fan, Y. Ren, J. Li, C. Yue, H. Jiang, Enhanced activity and enantioselectivity of henry reaction by the postsynthetic reduction modification for a chiral

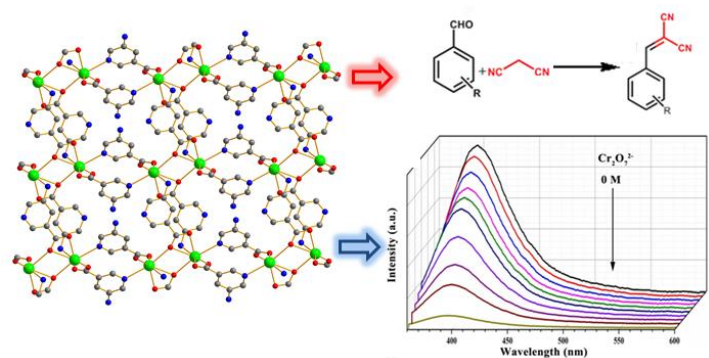
- Cu(salen)-based metal–organic framework, *Inorg. Chem.* 57 (2018) 11986–11994.
- [17] M. B. Majewski, A. J. Howarth, P. Li, M. R. Wasielewski, J. T. Hupp, O. K. Farha, Enzyme encapsulation in metal–organic frameworks for applications in catalysis, *CrystEngComm* 19 (2017) 4082–4091.
- [18] G. Zhu, M. Zhang, Y. Bu, L. Lu, X. Lou, L. Zhu, Enzyme-embedded metal–organic framework colloidosomes *via* an emulsion-based approach, *Chem. Asian J.* 13 (2018) 2891–2896.
- [19] X. Lian, Y. Huang, Y. Zhu, Y. Fang, R. Zhao, E. Joseph, J. Li, J.-P. Pellois, H.-C. Zhou, Enzyme-MOF nanoreactor activates nontoxic paracetamol for cancer therapy, *Angew. Chem., Int. Ed.* 57 (2018), 5725–5730.
- [20] D. Zhang, Z.-Z. Xue, J. Pan, M.-M. Shang, Y. Mu, S.-D. Han, G.-M. Wang, Solvated lanthanide cationic template strategy for constructing iodoargentates with photoluminescence and white light emission, *Cryst. Growth Des.* 18 (2018) 7041–7047.
- [21] Y. Wang, S.-H. Xing, F.-Y. Bai, Y.-H. Xing, L.-X. Sun, Stable lanthanide–organic framework materials constructed by a triazolylcarboxylate ligand: multifunction detection and white luminescence tuning, *Inorg. Chem.* 57 (2018) 12850–12859.
- [22] Y.-W. Peng, R.-J. Wu, M. Liu, S. Yao, A.-F. Geng, Z.-M. Zhang, Nitrogen coordination to dramatically enhance the stability of In-MOF for selectively capturing CO₂ from a CO₂/N₂ mixture, *Cryst. Growth Des.* 19 (2019) 1322–1328.
- [23] X.-N. Wang, N.-N. Mao, Y.-L. Bai, G.-L. Zhuang, B. Li, Two self-interpenetrating copper(II)-paddlewheel metal–organic frameworks constructed from bifunctional triazolate–carboxylate linkers, *Cryst. Growth Des.* 18 (2018) 6204–6210.
- [24] H.-Y. Liu, J. Liu, G.-M. Gao, H.-Y. Wang, Assembly of two metal-organic frameworks based on distinct cobalt dimeric building blocks induced by ligand modification: gas adsorption and magnetic properties, *Inorg. Chem.* 57 (2018) 10401–10409.
- [25] M. C. Wasson, J. Lyu, T. Islamoglu, O. K. Farha, Linker competition within a

- metal–organic framework for topological insights, *Inorg. Chem.* 58 (2019) 1513–1517.
- [26] J.-H. Liu, Y.-J. Qi, D. Zhao, H.-H. Li, S.-T. Zheng, Heterometallic organic frameworks built from trinuclear Indium and cuprous halide clusters: ligand-oriented assemblies and iodine adsorption behaviour, *Inorg. Chem.* 58 (2019) 516–523.
- [27] C. Chen, X. Feng, Q. Zhu, R. Dong, R. Yang, Y. Cheng, C. He, Microwave-assisted rapid synthesis of well-shaped MOF-74 (Ni) for CO₂ efficient capture, *Inorg. Chem.* 58 (2019) 2717–2728.
- [28] X.-D. Liu, Z.-L. Hou, Luminescent Tb(III)-based coordination polymer: selective detection of CS₂ and anti-tumor activity in cardiac myoma, *Inorg. Chem. Commun.* 95 (2018) 78–81.
- [29] Y. Wang, X. Wang, K. Zhang, X. Wang, X. Xin, W. Fan, F. Dai, Y. Han, D. Sun, Solvent-induced terbium metal–organic frameworks for highly selective detection of manganese(II) ions, *Dalton Trans.* 48 (2019) 2569–2573.
- [30] X.-L. Qu, B. Yan, Stable Tb(III)-based metal–organic framework: structure, photoluminescence, and chemical sensing of 2-thiazolidinethione-4-carboxylic acid as a biomarker of CS₂, *Inorg. Chem.* 58 (2019) 524–534.
- [31] S. Chen, Z. Shi, L. Qin, H. Jia, H. Zheng, Two new luminescent Cd(II)-metal-organic frameworks as bifunctional chemosensors for detection of cations Fe³⁺, anions CrO₄²⁻, and Cr₂O₇²⁻ in aqueous solution, *Cryst. Growth Des.* 17 (2017) 67–72.
- [32] Z. Han, L. Qi, G. Shen, W. Liu, Y. Chen, Determination of chromium(VI) by surface plasmon field-enhanced resonance light scattering, *Anal. Chem.* 79(2007) 5862–5868.
- [33] L. Hu, G.-X. Hao, H.-D. Luo, C.-X. Ke, G. Shi, J. Lin, X.-M. Lim, U. Y. Qazi, Y.-P. Cai, Bifunctional 2D Cd(II)-based metal–organic framework as efficient heterogeneous catalyst for the formation of C–C bond, *Cryst. Growth Des.* 18 (2018) 2883–2889.
- [34] T. K. Pal, D. De, S. Neogi, P. Pachfule, S. Senthilkumar, Q. Xu, P. K. Bharadwaj,

- Significant gas adsorption and catalytic performance by a robust Cu^{II}-MOF derived through single-crystal to single-crystal transmetalation of a thermally less-stable Zn^{II}-MOF, *Chem. Eur. J.* 21 (2015) 19064–19070.
- [35] Synthesis of {Pb(AIA)₂}_n (**1**): A mixture of Pb(OAc)₂ (0.1 mmol), HAIA (0.18 mmol), and 0.2 mL of LiOH (0.1 M) was dissolved in CH₃CN (2.5 mL) and H₂O (1.75 mL), which was continuously heated at 125 °C for 2 days in a Teflon-lined stainless steel vessel under autogenous pressure. The mixture was slowly cooled to indoor temperature. The block single crystals were directly collected and washed by fresh MeCN, which was dried in air with 59% yield based on Pb(OAc)₂. Anal. Calcd for C₁₂H₁₀O₄N₄Pb: C, 30.0; H, 2.1; N, 11.6 %. Found: C, 29.9; H, 2.0; N, 11.7 %.
- [36] Crystal data of C₁₂H₁₀O₄N₄Pb: $F_w = 646.9(2)$, triclinic, $P\bar{1}$, $a = 6.6657(12)$, $b = 8.7149(15)$, $c = 11.368(2)$ Å, $\alpha = 93.503(3)$, $\beta = 100.069(2)$, $\gamma = 93.963(2)$ °, $V = 646.9(2)$ Å³, $Z = 2$, $D_c = 2.472$ g cm⁻³, $\mu = 13.064$ mm⁻¹, $R(\text{int}) = 0.0132$, $N_{\text{ref}} = 2982$, $R_1 = 0.0202$, $wR_2 = 0.0500$ [$I > 2\sigma(I)$], $R_1 = 0.0214$, $wR_2 = 0.0505$ [all data], Goodness-of-fit on $F^2 = 1.038$. Large single crystal data for MOF **1** was directly collected on a Bruker SMART CCD diffractometer based on a graphite monochromated Mo K_α ($\lambda = 0.71073$ Å) at room temperature. The crystal structures were successfully analysed and refined using a direct and full-matrix least squares method on F^2 with anisotropic thermal parameters for non-hydrogen atoms (*SHELXL-2015*)^[44,45] through *OLEX2* interface program^[46].
- [37] W. Jiang, J. Yang, Y.-Y. Liu, S.-Y. Song, J.-F. Ma, A stable porphyrin-based porous metal-organic framework as an efficient solvent-free catalyst for C–C bond formation, *Inorg. Chem.* 56 (2017) 3036–3043.
- [38] Y. Zhang, Y. Wang, L. Liu, N. Wei, M.-L. Gao, D. Zhao, Z.-B. Han, Robust bifunctional lanthanide cluster based metal-organic frameworks (MOFs) for tandem Deacetalization–Knoevenagel reaction, *Inorg. Chem.* 57 (2018) 2193–2198.
- [39] X.-S. Wang, J. Liang, L. Li, Z.-J. Lin, P. P. Bag, S.-Y. Gao, Y.-B. Huang, R. Cao, An anion metal-organic framework with Lewis basic sites-rich toward

- charge-exclusive cationic dyes separation and size-selective catalytic reaction, *Inorg. Chem.* 55 (2016) 2641–2649.
- [40] X. Luo, X. Zhang, Y. Duan, X. Wang, J. Zhao, A novel luminescent Pb(II)-organic framework exhibiting a rapid and selective detection of trace amounts of NACs and Fe^{3+} with excellent recyclability, *Dalton Trans.* 46 (2017) 6303–6311.
- [41] F. Guo, Z. Chu, M. Zhao, B. Zhu, X. Zhang, Anion-templated assembly of three metal-organic frameworks with diverse structures for highly selective detection of $\text{Cr}_2\text{O}_7^{2-}$ and Fe^{3+} in aqueous solution, *J. Solid State Chem.* 274 (2019) 92–99.
- [42] S.-F. Tang, X. Hou, A highly stable dual functional zinc phosphite carboxylate as luminescent sensor of Fe^{3+} and $\text{Cr}_2\text{O}_7^{2-}$, *Cryst. Growth Des.* 19 (2019) 45–48.
- [43] J.-X. Li, D. Liu, Z.-C. Hao, G.-H. Cui, An unusual (3,4,5)-connected 3D cadmium metal-organic framework as a luminescent sensor for detection of $\text{Cr}_2\text{O}_7^{2-}$ in water, *Inorg. Chem. Commun.* 97 (2018) 79–82.
- [44] G. M. Sheldrick, A short history of *SHELX*, *Acta Cryst. A* 64 (2008) 112–122.
- [45] G. M. Sheldrick, Crystal Structure Refinement with *SHELXL*, *Acta Cryst. C* 71 (2015) 3–8.
- [46] O. V. Dolomanov, L. J. Bourhis, R. J. Gildea, J. A. K. Howard, H. Puschmann, *OLEX2*: a complete structure solution, refinement and analysis program, *J. Appl. Cryst.* 42 (2009) 339–341.

Graphical Abstract-Pictogram



This work presents a bi-functional 3D Pb^{II}-organic framework for Knoevenagel condensation reaction and highly selective luminescent sensing of Cr₂O₇²⁻. In addition, the resultant sample has excellent recyclability.

Highlights

1. A bi-functional 3D Pb^{II}-based MOF is successfully constructed.
2. It is an excellent catalysis for Knoevenagel condensation reaction.
3. It exhibits outstandingly selective luminescent sensing toward Cr₂O₇²⁻.

ACCEPTED MANUSCRIPT